

Spatio-temporal evolution and prediction of carbon storage in Kunming based on PLUS and InVEST models

Yimin Li^{1, 2}, Xue Yang^{1, 2}, Bowen Wu¹, Juanzhen Zhao³, Wenxue Jiang¹, Xianjie Feng³, Yuanting Li³

¹ School of Earth Sciences, Yunnan University, Kunming City, Yunnan, China

² Yunnan Provincial University Domestic High Score Satellite Remote Sensing Geological Engineering Research Center, Kunming City, Yunnan, China

³ Institute of International Rivers and Ecological Security, Yunnan University, Kunming City, Yunnan, China

Corresponding Author: Xue Yang

Email address: yx9912130@163.com

Carbon storage is a key ecosystem service of terrestrial environmental systems, which can effectively alleviate regional carbon emissions and is important for achieving carbon neutrality and peaking carbon emissions. We conducted a study in Kunming and analyzed the land utilization data for 2000, 2010, and 2020. We assessed the features of land utilization conversion and forecasted land utilization under three development patterns in 2030 on the basis of the PLUS model. We used the InVEST model to estimate the changes in the trend of carbon storage under three development scenarios in 2000, 2010, 2020, and 2030 and to determine the impact of socio-economic factors and natural factors on carbon storage. The results of the study indicated that (1) Carbon storage is intimately associated with land utilization practices. Carbon storage in Kunming in 2000, 2010, and 2020 was 1.146×10^8 t, 1.139×10^8 t, and 1.120×10^8 t, respectively. During the 20 years, forest land decreased by 142.28 km², and the decrease in forest land area caused loss of carbon storage. (2) The carbon storage under the trend continuation scenario, Eco-friendly scenario, and comprehensive development scenario in 2030 was predicted to be 1.102×10^8 t, 1.136×10^8 t, and 1.105×10^8 t, respectively, indicating that implementing ecological protection and cultivated land protection measures can facilitate regional ecosystem carbon storage restoring. (3) For the study area, Impervious surfaces and vegetation have the greatest degree of influence on carbon storage. A spatial global and local negative correlation was found between impervious surface coverage and ecosystem carbon storage. A spatial global, and local positive correlation was found between NDVI and ecosystem carbon storage. Therefore, ecological and farmland protection policies need to be strengthened, the expansion of impervious surfaces should be strictly controlled, and vegetation coverage should be improved.

1 Spatio-temporal evolution and prediction of carbon 2 storage in Kunming based on PLUS and InVEST 3 models

4 Yimin Li^{1,2,#}, Xue Yang^{1,#}, Bowen Wu¹, Juanzhen Zhao³, Wenxue Jiang¹, Xianjie Feng³,
5 Yuanting Li³

6 ¹ Yunnan University, School of Earth Sciences, Kunming, Yunnan, China

7 ² Yunnan Provincial University Domestic High Score Satellite Remote Sensing Geological
8 Engineering Research Center, Kunming, Yunnan, China.

9 ³ Yunnan University, Institute of International Rivers and Ecological Security, Kunming,
10 Yunnan, China

11

12 Corresponding Author:

13 Xue Yang¹

14 Wu Jiaying Street, Kunming, Yunnan, 650500, China

15 Email address: yx9912130@163.com

16 #Contributed equally to this work.

17

18 Abstract

19 Carbon storage is a key ecosystem service of terrestrial environmental systems, which can
20 effectively alleviate regional carbon emissions and is important for achieving carbon neutrality
21 and peaking carbon emissions.

22 We conducted a study in Kunming and analyzed the land utilization data for 2000, 2010, and
23 2020. We assessed the features of land utilization conversion and forecasted land utilization
24 under three development patterns in 2030 on the basis of the PLUS model. We used the InVEST
25 model to estimate the changes in the trend of carbon storage under three development scenarios
26 in 2000, 2010, 2020, and 2030 and to determine the impact of socio-economic factors and natural
27 factors on carbon storage.

28 The results of the study indicated that (1) Carbon storage is intimately associated with land
29 utilization practices. Carbon storage in Kunming in 2000, 2010, and 2020 was 1.146×10^8 t,
30 1.139×10^8 t, and 1.120×10^8 t, respectively. During the 20 years, forest land decreased by
31 142.28 km^2 , and the decrease in forest land area caused loss of carbon storage. (2) The carbon
32 storage under the trend continuation scenario, Eco-friendly scenario, and comprehensive
33 development scenario in 2030 was predicted to be 1.102×10^8 t, 1.136×10^8 t, and 1.105×10^8
34 t, respectively, indicating that implementing ecological protection and cultivated land protection
35 measures can facilitate regional ecosystem carbon storage restoring. (3) For the study area,
36 Impervious surfaces and vegetation have the greatest degree of influence on carbon storage. A
37 spatial global and local negative correlation was found between impervious surface coverage and
38 ecosystem carbon storage. A spatial global, and local positive correlation was found between
39 NDVI and ecosystem carbon storage. Therefore, ecological and farmland protection policies

40 need to be strengthened, the expansion of impervious surfaces should be strictly controlled, and
41 vegetation coverage should be improved.

42 **Introduction**

43 Due to rapid urbanization and industrialization, almost all cities around the world have
44 experienced several climate-related and environmental problems (Cao, 2019; Sarkodie et al.,
45 2020), such as acid rain and the greenhouse effect, which are linked to the increasing intensity of
46 land utilization by humans (Xu et al., 2018). Carbon dioxide strongly influences the climate.
47 Greenhouse gases such as carbon dioxide emitted in unusually large quantities due to human
48 activities are the dominant causes of global warming and aggravate climate instability (Gao et
49 al., 2022; Yang et al., 2022; Zhang et al., 2022). Carbon dioxide can be stored in vegetation and
50 soil, which decreases the atmospheric carbon dioxide content (Dorendorf et al., 2015). The
51 storage of carbon is vital for regulating the climate and is an important ecosystem service
52 function. China is the world's top carbon emitter. At the 75th session of the United Nations
53 General Assembly (2020), China pledged that it will aim to reach the peak of carbon emissions
54 by 2030 and achieve carbon neutrality by 2060 (Chen et al., 2022).

55 Kunming is a vital city of Yunnan Province in China, and the main population and GDP of
56 Yunnan Province are concentrated in this city. It is the most important center for the economic
57 development of the province and is an essential corridor for economic and cultural
58 communications between China and Southeast Asian countries. Additionally, Kunming has rich
59 forest resources and biodiversity, and thus, is a vital area in the Yangtze River Economic Belt
60 and an Eco-conservation shield in the upstream of the Yangtze River. In October 2021, The 15th
61 Conference of the Parties (COP15) of the UN Convention on Biological Diversity was hosted in
62 Kunming. At the conference, new ideas were presented for conserving worldwide biodiversity.
63 During the 14th five-year plan period of China's national economic and social development,
64 Yunnan Province pledged that it would strive "to become the vanguard of China's ecological
65 civilization construction" as a long-term goal and incorporate the aim to achieve "peaking carbon
66 emissions and carbon neutrality" into the general arrangement of economic development and the
67 establishment of an Eco-civilization. To realize these goals, Yunnan should promote the
68 establishment of an Eco-civilization, which is not only a significant embodiment of Yunnan's
69 initiative to serve the national developmental strategy, but also an important embodiment of
70 integrating into the national development. Therefore, studying and forecasting the response of
71 land utilization conversions to carbon storage in Kunming can help build a strong ecological
72 security barrier in southwest China and provide theoretical support for reducing regional
73 emissions.

74 The emission of large amounts of greenhouse gases poses a serious threat to the global
75 climate and environment. Several studies in the field of the ecological environment have
76 estimated regional carbon storage and carbon emissions (Cai and Peng, 2021; Gogoi et al., 2022;
77 Li et al., 2022). Carbon storage is mainly estimated by traditional estimation methods and model
78 methods. Traditional estimation methods, such as the sample inventory (Li et al., 2021) and the
79 ecosystem carbon flux monitoring (Yang et al., 2022), evaluation models include CASA (Tong

80 et al., 2016), Bookkeeping (Kong et al., 2018), InVEST (Zhang et al., 2022a), etc. The traditional
81 estimation method is only suitable for small-area carbon storage research due to its large
82 workload and low efficiency. The InVEST model is broadly applicable to the field of carbon
83 sequestration research (Chen et al., 2021; Wang et al., 2022; Zhang et al., 2022a; Zhao et al.,
84 2022) because it demands a small amount of data, has high speed of operation, and performs
85 convenient space-time visualization. Studying the current space-time characteristics of carbon
86 storage and predicting future variations in land use and carbon storage can help in realizing the
87 'double carbon' goal. Several researchers have investigated prospective land utilization and
88 carbon storage prediction at different scales. With the FLUS and InVEST models, Shao et al.
89 (2022) predicted the evolution of Beijing's carbon storage in 2035 under natural evolution
90 scenario, population evacuation urban development scenario, and green intensive ecological
91 protection scenario. They also conducted zoning management studies based on spatial
92 autocorrelation models. Li et al. (Li et al., 2020) applied the SEUTH model to estimate the urban
93 growth of Wuhan under different scenarios in 2030 and determined the consequences of urban
94 sprawl on local carbon storage in combination with the InVEST model. Using the PLUS and
95 InVEST models, Rukeya et al. (2022) dynamically evaluated the characteristics of land
96 utilization and carbon storage varies in city cluster on the northern slope of Tianshan Mountains
97 under different scenarios from 2000 to 2030. Ding et al. (2022) utilized the PLUS and InVEST
98 models to investigate and predict evolution in land-use and carbon storage around the Hangzhou
99 Bay since 2000 to 2018 and 2018 to 2030.

100 The models used to mimic futuristic land utilization/land cover mainly include CA-Markov
101 (Song et al., 2022), FLUS (Xie et al., 2022), SD (Zhang et al., 2020b), PLUS (Yang et al., 2022),
102 etc. Among them, the patch-level land use simulation model (PLUS) is a relatively new land
103 utilization/land cover forecast model. By mining various driving factors, using the land
104 expansion analysis strategy (LEAS), the random forest algorithm was used to obtain the
105 development possibility of each category (Liang et al., 2021) to simulate the future changes in
106 land use patches with greater accuracy in different years and different environments. The
107 Markov model has higher accuracy in predicting quantities (Zhao et al., 2022). The integration of
108 the PLUS model with the Markov model allows for better estimation of regional land
109 utilization/land cover at different future development scenarios.

110 Several studies have predicted the space-time development in regional carbon storage by the
111 model method. Therefore, in this study, we selected Kunming City in Yunnan Province as the
112 study area taking the three-period land use raster dataset and driving factors during 2000 to 2020
113 as the basis. The goals of this study were as follows: (1) Based on the PLUS model, the land-use
114 pattern under different development patterns in Kunming City in 2030 was predicted, and the
115 land utilization transformation trend since 2000 to 2030 was analyzed. (2) The InVEST model
116 was adopted to assess the time-space distribution and change of carbon storage in Kunming from
117 2000 to 2030 and determine the influential effect of land using on carbon storage in different
118 periods. (3) The spatial correlation and influencing factors of carbon storage were analyzed to

119 deliver a strong scientific foundation for achieving the goal of peaking carbon emissions and
120 carbon neutralization on a geographical level.

121 **Materials & Methods**

122 **Study area**

123 Kunming is directly northeast of central Yunnan Province (102°10' ~ 103°40' E, 24°23' ~ 26°22'
124 N) in the central Yunnan-Guizhou Plateau (Fig. 1) (Fang et al., 2021), is the administrative,
125 commercial, and cultural center of Yunnan Province. The city has seven districts, three counties,
126 one county-level city, and three autonomous regions. In 2021, Kunming had a permanent
127 population of 8.520 million. The land area of Kunming is about 21,011.41 km², and the
128 elevation of the terrain decreases from north to south. The area has a low latitude highland
129 monsoon climate, affected by the southwest monsoon of the Indian Ocean. The temperature is
130 mild, winters are not very cold, and summers are not very hot, which is why this place is called
131 'Spring City'. Kunming is positioned in the southwest borderland of China and forms a
132 connection between Southeast Asia and South Asia. It also acts as an overwhelming safe
133 ecological barrier in southwest China. The city aims to become a model city of ecological
134 civilization.

135 **Data sources and preprocessing**

136 The main data used for this research mainly included land utilization data, carbon density,
137 driving factors, and other data. (1) Land utilization data: The land-use data (30 m × 30 m) was
138 obtained from the Resource and Environmental Science and Data Center of the Chinese
139 Academy of Sciences. The data were selected in time: 2000, 2010 and 2020, and the geographic
140 coordinate system used was GCS _ WGS _ 1984, which included 25 secondary land types and
141 six primary land types (cultivated land, forest land, grassland, water area, construction land, and
142 unused land). (2) Carbon density: The carbon density varies by land use types. The studies which
143 had similar levels of natural resources (Ke and Tang, 2019) and climatic conditions (Yan et al.,
144 2015; Tang et al., 2019) to that in the study area were selected as references. Then, the data were
145 corrected according to the above-ground carbon density dataset of the terrestrial ecosystem of
146 China in 2010 and the carbon density dataset of soil in 0 ~ 100 cm of the terrestrial ecosystem of
147 China in 2010. Finally, the carbon density dataset for land utilization categories in Kunming was
148 obtained (Table 1). (3) Driving factors: The driving factor data for future land prediction
149 included physical factors and social factors. The physical factors involved the DEM, slope,
150 annual average rainfall, soil type, annual average temperature, and distance to the water system.
151 The social factors included the GDP, distance to the government office, distance to the highway,
152 distance to the main road (first-class road and second-class road), population density, data
153 source, and resolution, as shown in Table 2. Next, ArcGIS was used to unify the resolution to 30
154 m × 30 m, and unified the geographic coordinate system to GCS _ WGS _ 1984. (4) Other data:
155 Four Landsat 8 OLI and TIRS images in August 2020 were selected for radiometric calibration,
156 atmospheric correction, splicing, and cropping to obtain remote sensing images of Kunming
157 City, to extract the impervious surface in 2020. NDVI was directly obtained from the vegetation
158 index data MOD13A1.

159 **Methods**

160 The research framework was composed of four stages (Fig. 2). (1) Data preparation and
 161 preprocessing. (2) Based on the PLUS model, the land utilization changes under the trend
 162 continuation situation, Eco-friendly scenario, and comprehensive development scenario were
 163 predicted for 2030. (3) With the InVEST model, the space-time allocation of carbon storage
 164 under different development scenarios was evaluated from 2000 to 2030, and the tendency of
 165 land use revolution in the study area from 2000 to 2030 was discovered to determine the impact
 166 of land utilization variation on carbon sink. (4) The spatial correlation of carbon storage was
 167 evaluated using the spatial autocorrelation model, and the influencing factors of carbon storage
 168 were analyzed.

169 **Ecosystem carbon storage estimation**

170 In this study, the Carbon Storage and Sequestration module of the InVEST model was used to
 171 calculate the carbon storage in Kunming. The basic assumption of this module is that the value
 172 of the carbon density of a specific land category is fixed, and the carbon storage of that land type
 173 can be acquired by multiplying the value of carbon density with that of the land area (Gong et al.,
 174 2022). The carbon storage module in the InVEST model divides the ecosystem carbon storage
 175 into four basic carbon pools (Lin et al., 2022), which include the terrestrial biogenic carbon,
 176 subsurface biogenic carbon, soil carbon, and dead organic carbon. The sum of the carbon stock
 177 of the four carbon pools provides the value for the total carbon storage of the ecosystem in the
 178 area, which can be achieved using equations (1) and (2) (Li et al., 2020).

$$179 \quad C_i = C_{i- above} + C_{i- below} + C_{i- soil} + C_{i- dead} \quad (1)$$

$$180 \quad C_{tot} = \sum_{i=1}^n C_i \times S_i \quad (2)$$

181 Here, C_i indicates the carbon density of land utilization type i ; $C_{i- above}$, $C_{i- below}$, $C_{i- soil}$,
 182 and $C_{i- dead}$ indicate the carbon density of terrestrial biogenic carbon, subsurface biogenic
 183 carbon, soil carbon, and dead organic carbon of land use type i , respectively; C_{tot} indicates the
 184 total carbon storage in the region; S_i indicates the area of land utilization pattern i ; n indicates the
 185 total number of land use types.

186 **Future Land Use Prediction and Scenario Setting**

187 (1) PLUS model

188 In this study, the PLUS model was utilized to forecast land utilization in Kunming under distinct
 189 growth scenarios in 2030. The PLUS model is a new land use prediction model proposed by Xun
 190 et al. (China University of Geosciences). Compared to other traditional prediction models, it has
 191 improved emulation capability and can measure the landscape pattern more precisely (Yang et
 192 al., 2022). The PLUS model mainly combines the land expansion analysis strategy (LEAS) and
 193 the CA model with multi-type random patch seeds (CARS). The LEAS module is employed to
 194 extract the land cover expansion, and then, the random forest classification algorithm is utilized
 195 to mine the probability of change and inertia of each land use type (Gao et al., 2022). The CARS
 196 module affects the local land contestation process through a self-adaptive coefficient and drives
 197 the changes in land utilization intensity to meet the upcoming land use demand. For forecasting

198 the number of prospective land application patches, a Markov model with high simulation
199 accuracy is selected (Sun and Liang, 2021).

200 (2) Scenario Setting

201 The development planning and the land use change of Kunming City are affected by many
202 factors. The previous planning of Kunming City started in 2006 and ended in 2020. The next
203 overall planning of land and space in Kunming City started in 2021 and is planned till 2035;
204 2030 is the intermediate node of the next land and space planning of Kunming City.
205 Additionally, following the implementation outline of "Kunming City building regional
206 international center city (2017–2030)" issued in September 2017, Kunming City will be fully
207 transformed into a regional international center city in southwest China in 2030. Therefore, in
208 this study, we selected 2030 as the prediction year of future land use in Kunming.

209 In accordance with the historical law of land utilization change in Kunming, along with the
210 development situation and future planning, and assuming that the region can meet the future
211 natural, social, and economic needs, the PLUS model was used to construct three scenarios (Cui
212 et al., 2022; Ding et al., 2021; Zhang and Gu, 2022) for the coming land utilization expansion of
213 Kunming. These scenarios are as follows:

214 1) Trend continuation scenario (S1). According to the law of land utilization change in Kunming
215 between 2010 and 2020, only the water area can be controlled as the restricted conversion area,
216 and the construction land cannot be transferred to alternative land types. Using the Markov
217 model, the land use types of Kunming in the 2030 trend continuation scenario were predicted.

218 2) Ecological protection scenario (S2). The Yunnan Province is committed to leading the
219 ecological civilization construction goals, guided by ecological and environmental protection, by
220 limiting the large extension of construction land, increasing the shift of other types of land to
221 woodland and grassland, and reducing the conversion of eco-land to unused land.

222 3) Comprehensive development scenario (S3). While ensuring economic development, the
223 protection of the ecosystem, substantially reducing the transfer of non-construction land to
224 construction land, and increasing the transfer probability of unused land to ecological land
225 without affecting economic development need to be considered. Since cultivated land is
226 economically important, the conservation policy of cultivated land needs to be considered to
227 strictly control the transformation of cultivated land.

228 The neighborhood weight reflects the expandability of a certain land utilization type. When
229 the value is closer to 1, the extension capacity of the land utilization type is stronger. Following
230 the law of land utilization conversion in Kunming for the period 2010-2020, and based on the
231 findings of published studies (La et al., 2021), the neighborhood weights of each land utilization
232 type under various scenarios were set by comparing the accuracy of the outcomes of simulation
233 based on different parameters (Table 3).

234 (3) Verifying the accuracy of the simulation

235 According to the land use data of Kunming City in 2010, the PLUS model was employed to
236 forecast the results of the land utilization type of Kunming City in 2020. By comparing the
237 simulated results with the real land use data in 2020, the Kappa coefficient of the two sets of data

238 was 0.8638, and the overall accuracy was 90.72%. The simulation accuracy was high, indicating
 239 that the model and various parameters might be used for simulating the land use of Kunming
 240 City in the future.

241 **Impervious surface extraction**

242 The impervious surface area (ISA) is a typical land cover type and an important indicator for
 243 measuring and analyzing city development and the ecology (Xu, 2009). The index method is
 244 generally adopted to extract the urban impervious surface. The representative spectral indices
 245 include the normalized building index (NDBI), the normalized difference impervious surface
 246 index (NDISI), and the enhanced normalized difference impervious surface index (ENDISI)
 247 (Duan et al., 2022). ENDISI can better identify shadows of mountains and remains unaffected by
 248 terrain factors while identifying impervious surfaces. Kunming City is dominated by
 249 mountainous terrain. Selecting this index for extracting information on impervious surfaces can
 250 prevent mountain shadows from affecting the extraction accuracy of impervious surfaces. The
 251 ENDISI can be calculated using Equation (3).

$$252 \quad \text{ENDISI} = \frac{(2\text{Blue} + \text{MIR}_2) \div 2 - (\text{NIR} + \text{Red} + \text{MIR}_1)}{(2\text{Blue} + \text{MIR}_2) \div 2 + (\text{NIR} + \text{Red} + \text{MIR}_1)} \quad (3)$$

253 Here, Blue, Red, NIR, MIR_1 , and MIR_2 are the reflectance of blue, red, near-infrared,
 254 shortwave infrared 1, and shortwave infrared 2 bands corresponding to the image.

255 Before extracting the information on the impervious surface, the normalized water index
 256 MNDWI (Xu, 2008) needs to be used to mask the large area of water and snow over the study
 257 area. The MNDWI index can be derived from the Equation (4).

$$258 \quad \text{MNDWI} = \frac{(\text{Green} - \text{MIR}_1)}{(\text{Green} + \text{MIR}_1)} \quad (4)$$

259 Here, Green, MIR_1 , and MIR_2 are the reflectance of green, shortwave infrared 1, and
 260 shortwave infrared 2 bands corresponding to the image, respectively.

261 Using ArcGIS, 700 verification points were randomly generated in the working area after
 262 masking water and snow. With the data on the impervious surface extracted from the Landsat 8
 263 image in 2020, the land use data and the remote sensing imagery of Kunming City in this period
 264 were selected, and the accuracy of the extracted impervious surface was determined by artificial
 265 visual interpretation. The Kappa coefficient was 0.7582, and the overall accuracy was 89.86%. It
 266 demonstrated that the accuracy of the impervious surface met the requirements of subsequent
 267 research.

268 **Results**

269 **Land-use change analysis**

270 From the overlay map of the area proportion of land utilization types (Fig. 3), we found that the
 271 land in Kunming City during 2000-2020 was mainly forest land, which covered about 45% of the
 272 total area studied. Since 2000 to 2020, the total area of forest land, grassland, and cultivated land
 273 decreased. The land use transfer matrix from 2000 to 2020 (Table 4) showed that forest land
 274 decreased by 142.28 km², grassland decreased by 328.95 km², and cultivated land decreased by
 275 278.07 km² in 20 years. The growth rate of construction land was high; construction land

276 increased by 708.84 km², and the area proportion increased from 2.3% to 5.7%. The
277 development process of S1 in 2030 was similar to the trend of 2000–2020. Woodland, grassland,
278 and cultivated land in 2030 decreased by 123.86 km², 150.61 km², and 197.358 km²,
279 respectively. However, construction land increased by 451.136 km², and water area and unused
280 land remained unchanged. In the S2 scenario, with ecological protection as the leading role, the
281 area of forest land increased by 1.1% and the growth rate of construction land slowed down. In
282 the S3 scenario, where cultivated land conservation policy and economic development were
283 considered, cultivated land and construction land increased by 55.82 km² and 209.28 km²,
284 respectively, while forest land and grassland decreased by 123.96 km² and 151.79 km²,
285 respectively.

286 The construction land in the four periods was concentrated in the main urban area of
287 Kunming (Wuhua District, Panlong District, Xishan District, Guandu District, and Chenggong
288 District) and the surrounding areas (eastern Anning City, northern Chongming County, and
289 northern Jinning District) (Fig. 4). According to the statistical yearbook of Yunnan Province in
290 2020, the main urban area of Kunming comprised 63.17% of the population and generated
291 73.76% of the GDP of the city. A large population and capital flow led to an increase in
292 construction, and ecological land, such as forest land and grassland, decreased considerably. The
293 land utilization types in Luquan County and Xundian County are mainly woodland and
294 grassland, which act as important ecological barriers in Kunming City. The Jiaozi Snow
295 Mountain Nature Reserve is in Luquan County and is an important water conservation ecological
296 reserve in Kunming City. The overall territorial spatial layout of Kunming is: the southern
297 Dianchi Lake basin is the core of economy and population, and the northern mountainous area is
298 the ecological security area.

299 **Analysis of space and time Variation of Ecosystem Carbon Storage**

300 The carbon storage in Kunming in 2000, 2010, and 2020 was 1.146×10^8 t, 1.139×10^8 t, and
301 1.120×10^8 t, respectively, indicating a continuous decrease, with a total decrease of
302 2.619×10^6 t in 20 years. The reduction of carbon storage in 2010–2020 was the highest, with a
303 decrease of 1.917×10^6 t. During this period, the economic development and urbanization of
304 Kunming were rapid and the demand for land use was relatively high.

305 In 2030, carbon storage is predicted to be 1.102×10^8 t in the S1, and the loss of ecosystem
306 carbon stock is greater. The ecosystem carbon storage might decrease by 1.818×10^6 t compared
307 to that in 2020. In 2030, carbon storage is predicted to be 1.136×10^8 t in the S2 scenario, which
308 is 1.601×10^6 t higher than that in 2020, indicating that ecological protection can restore
309 ecosystem carbon storage in Kunming. Finally, carbon storage in the S3 is predicted to be
310 1.105×10^8 t in 2030, and the ecosystem carbon storage might decrease by 1.479×10^6 t
311 compared to that in 2020, which is less than the carbon loss in the S1. As shown in Fig. 5, the
312 terrestrial biogenic carbon, subsurface biogenic carbon, dead organic carbon, and soil carbon in
313 the S2 scenario in 2030 are predicted to be higher than those in the S1 and S3 scenarios. The soil
314 carbon gap was found to be the largest, which was 1.539×10^6 t and 1.250×10^6 t higher than
315 the soil carbon in the S1 and S3 scenarios, respectively. The terrestrial biogenic carbon storage,

316 belowground carbon storage, and dead organic carbon storage in the S1 and S3 scenarios were
317 similar, while the soil carbon storage in S3 was higher than that in S1, which was consistent with
318 the changes in total carbon storage.

319 The overall content of ecosystem carbon stock in Kunming is high, showing a 'north high,
320 south low' distribution (Fig. 6 and 7). Carbon storage is mainly distributed in Luquan County,
321 Xundian County, and Yiliang County on the east and west of the research area, while the main
322 urban area of Kunming City in the south of the study area is highly urbanized and has lesser
323 quantities of stored carbon. From 2000 to 2030, the change in the spatial layout of carbon storage
324 in Kunming was mainly found to occur in the main urban area of Kunming. On the basis of our
325 findings using the S1 scenario, from 2000 to 2030, due to rapid urbanization, the construction
326 land in the main urban area expanded remarkably, resulting in the loss of regional ecosystem
327 carbon storage every year. Under the ecological protection-oriented development of the S2
328 scenario, in 2030, the carbon stock in the main urban area of Kunming increased compared to
329 that in 2020. When considering the cultivated land conservation policy, eco-friendly policy, and
330 economic development, carbon storage in the main urban area of Kunming was lower than that
331 in 2020, but the reduction range was narrower than that in the S1 scenario. The results showed
332 that carbon sequestration in the main urban area of Kunming can strongly affect the change in
333 the ecosystem carbon storage in the whole city.

334 **Effects of Land-Use Conversion on Carbon Storage**

335 Land utilization/land cover significantly affects vegetation cover and biomass and is also the
336 primary purpose for the distribution and change of carbon sequestration in regional terrestrial
337 ecosystems (Zhang et al., 2022b). The dynamic changes in carbon stock induced by the changes
338 in main land use types in Kunming from 2000 to 2030 are shown in Fig. 8. From 2000 to 2030,
339 according to the S1 scenario, carbon storage decreased mainly because of the shift from forest
340 land and grassland to other land use types. Although the policy of returning farmland to forest
341 has partly promoted the transfer of cultivated land to forest land, expansion of construction land
342 encroaches forest land, leading in a sharp decrease in the ecosystem carbon reserve. Under the
343 S2 scenario, in 2030, the increase in ecological lands, such as forest land and grassland, was
344 predicted to be the key reason for the increase in carbon sequestration. Under the S3
345 comprehensive development scenario, in 2030, the cultivated land conservation policy was found
346 to promote the increase in cultivated land carbon storage, while the forest land and grassland
347 carbon stock decreased. The carbon density of forest land and grassland was higher than that of
348 cultivated land, resulting in a decrease in the overall ecosystem carbon storage. The outcomes
349 suggested that the conversion in land utilization type is consistent with the changes in the
350 ecosystem carbon stock, and land use/land cover directly affects ecosystem carbon sequestration.

351 **Spatial Correlation Analysis of Ecosystem Carbon Storage**

352 Spatial correlation is segmented into spatial global autocorrelation and spatial local
353 autocorrelation (Luo et al., 2022). In this study, Moran's I index was employed to represent the
354 spatial global autocorrelation of ecosystem carbon storage in Kunming (Xiong et al., 2021) and
355 Getis-Ord G_i^* was employed to measure the spatial local autocorrelation (Zhang et al., 2020a).

356 In this study, Kunming was divided into a 2 km × 2 km grid, and the carbon storage data in the
357 three development scenarios for 2000–2020 and 2030 were linked to the grid. Based on this
358 scale, the spatial correlation of carbon stock in Kunming was analyzed.

359 Regarding global autocorrelation, the spatial Moran's I values of carbon storage in Kunming
360 were 0.5583 in 2000, 0.5546 in 2010, 0.5635 in 2020, 0.5900 in 2030 S1, 0.5672 in 2030 S2, and
361 0.5763 in 2030 S3, respectively (all values were greater than 0), indicating a significant spatial
362 global autocorrelation in carbon storage in Kunming. For local autocorrelation, the results of the
363 carbon storage hotspot analysis under the three development scenarios in Kunming from 2000 to
364 2030 are shown in Fig. 9. From 2000 to 2020, the area designated as the hotspot of carbon stock
365 in Kunming reduced, while the area considered to be a coldspot increased. Except for the
366 northeast of Dongchuan District, the coldspot area in other areas, especially in the main urban
367 area of Kunming, increased. In the last 20 years, the hotspots of carbon stock in the research area
368 were scattered in the northwestern, western, central, and eastern regions, including the east and
369 west sides of Luquan County, Xishan District, the western part of Chongming County, the
370 northern part of Yiliang County, and the eastern part of Guandu District. Carbon storage was not
371 only higher in these areas but high-value areas of carbon sequestration were also gathered in
372 these areas, primarily situated in zones with less construction land, excellent plant coverage, and
373 more ecological land. The coldspot area was mostly distributed in the northeastern, central, and
374 southern locations of Kunming, i.e., the northeastern part of Dongchuan District, the eastern part
375 of Chongming County, the eastern part of Yiliang County, the northern and western parts of
376 Shilin County, and the central part of the main urban area of Kunming City. These areas
377 underwent rapid land development, had complex topography and geomorphology, and
378 fragmented distribution of ecological land, forming an area with low carbon storage. In the S1
379 scenario, in 2030, the coldspot area in the main urban areas of Anning City and Kunming City
380 increased. The coldspot area in the S2 scenario was slightly smaller compared to 2020 in the
381 main urban area. The coldspot area in the S3 scenario, in 2030, was similar to that in 2020,
382 indicating that the eco-friendly and cultivated land protection policies were beneficial to
383 moderate the loss of ecosystem carbon sequestration in Kunming City.

384 **Research on Driving Factors of Ecosystem Carbon Storage**

385 **Correlation between Ecosystem Carbon Storage and Impact Factors**

386 Based on the spatial-temporal allocation and variation of carbon stock in Kunming, in this study,
387 we performed correlation analysis (Chen et al., 2022; Zhang et al., 2022) to determine the effects
388 of natural factors and socio-economic factors on carbon storage. Taking the data on impact
389 factors and carbon storage in 2020 as an example, the data were set to a grid of 2 km × 2 km
390 according to the study area using the grid method. In total, 5,153 grid points were generated. The
391 impact factors included impervious surface coverage, GDP, population density, altitude, NDVI,
392 and annual average precipitation.

393 The results of Pearson's correlation coefficient analysis between carbon storage and various
394 influencing factors in Kunming are shown in Table 5. Carbon storage was moderately negative
395 correlated with impervious surface coverage, weakly negatively correlated with GDP and

396 population density, strongly positively correlated with NDVI, and weakly positively correlated
397 with altitude and annual rainfall. The results showed that at a grid scale of $2 \text{ km} \times 2 \text{ km}$,
398 impervious surface and vegetation had the greatest impact on carbon storage in Kunming, and
399 carbon storage was negatively correlated with impervious surface coverage and positively
400 correlated with NDVI.

401 **Bivariate spatial autocorrelation analysis of carbon storage and the influencing factors**

402 Depending on the results of Pearson's correlation analysis, two indicators that had the strongest
403 relevance with the carbon storage of the ecosystem in Kunming were selected, i.e., impervious
404 surface coverage and NDVI, and bivariate spatial autocorrelation analyses were performed
405 between the two indicators and carbon storage data. The bivariate global spatial autocorrelation
406 is represented by the bivariate 'Moran's I index. The bivariate 'Moran's I index of impervious
407 surface coverage and ecosystem carbon storage was -0.379 . The negative value of 'Moran's I
408 index indicated a global negative correlation between impervious surface coverage and
409 ecosystem carbon storage. The bivariate 'Moran's I index of NDVI and ecosystem carbon
410 storage was 0.450 . The positive value of 'Moran's I index indicated that there was a global
411 positive correlation between NDVI and ecosystem carbon storage.

412 The bivariate LISA cluster map of impervious surface coverage and carbon storage of the
413 ecosystem in Kunming, which reflects the local agglomeration characteristics of the two in
414 space, is shown in Fig. 10a. The impervious surface coverage and carbon storage of the
415 ecosystem showed opposite values of the two-pole agglomeration characteristics in space, which
416 mainly were high-low agglomeration and low-high agglomeration, i.e., carbon stock in the area
417 with low impervious surface coverage was higher, and carbon stock in the area with high
418 impervious surface coverage was lower. The bivariate LISA clustering results of NDVI and
419 ecosystem carbon storage in Kunming (Fig. 10b) showed that NDVI and ecosystem carbon
420 storage had a similar value for the polar agglomeration characteristics in space, mainly high-high
421 agglomeration and low-low agglomeration. Thus, the regional ecosystem carbon storage with
422 higher vegetation coverage was higher, and the regional ecosystem carbon storage with lower
423 value coverage was lower. These results suggested a local negative correlation between
424 impervious surface coverage and ecosystem carbon storage and a local positive correlation
425 between NDVI and ecosystem carbon storage.

426 **Discussion**

427 **Contribution of Land Use Driving Factors**

428 Social and natural factors mainly drive land use change (Gong et al., 2022). Social factors
429 include population density, GDP, distance to road, distance to the government office, etc. Natural
430 factors include terrain factors, such as slope and elevation, and climatic factors, such as mean
431 annual rainfall and mean annual temperature. In this study, 11 driving factors of social economy
432 and climate were selected to forecast land utilization in 2030, and the contribution of each
433 driving factor was evaluated (Table 6). A higher contribution of a factor indicated a greater
434 impact of the driving factor on local land use evolution.

435 The driving factors with the highest contribution to cultivated land were GDP (0.166), DEM
436 (0.111), and population density (0.104). Cultivated land expansion is inextricably linked to
437 population and economic development because rapid population and economic growth will lead
438 to greater food demand (Liao et al., 2021). Climatic conditions were different at different
439 altitudes. Agricultural farming was closely related to climatic conditions, and thus, cultivated
440 lands were generally distributed in low-altitude suitable farming areas. The driving factors with
441 the highest contribution to forest land were DEM (0.183), population density (0.125), and slope
442 (0.117). The altitude and slope were important topographic factors affecting vegetation growth.
443 Generally, areas that have a small slope and are at a low altitude are more suitable for the growth
444 of vegetation. Areas with a higher population density have less forest land area, and population
445 density partly limits the expansion of forest land. The driving factors with the highest
446 contribution to grassland were GDP (0.133), population density (0.117), and distance to the
447 water system (0.104). The GDP and population density restricted grassland expansion, while the
448 water system promoted grassland expansion. The area closer to the water system was more prone
449 to grassland expansion. The driving factors with the highest contribution to construction land
450 were population density (0.154), GDP (0.143), and the mean annual temperature (0.122). A
451 greater population density and a higher GDP were associated with a greater demand for and
452 more expansion of construction land. The mean annual temperature affected the development of
453 construction land by changing the population density. The driving factors with the highest
454 contribution to the unused land were DEM (0.306), the mean annual temperature (0.199), and the
455 mean annual rainfall (0.156). The climate in high-altitude areas is harsh, and the perennial
456 temperature is low, which is unfavorable for vegetation growth and human habitation.

457 **Suggestions on Carbon Sink Function Restoration and Governance**

458 The period from 2000 to 2020 was an important stage of economic development in Kunming. In
459 the last 20 years, the gross domestic product increased from 6,262.853 million yuan to
460 67,337.909 million yuan, the population increased from 4.8094 million to 8.463 million, and the
461 construction land expanded from 484.21 km² to 1193.05 km². The area of forest land and
462 grassland decreased considerably, resulting in a decline in ecosystem carbon storage in Kunming
463 in the last 20 years. Based on the predictions of the trend continuation scene, ecological
464 protection scene, and comprehensive development scenario, taking timely measures to protect
465 the ecosystem is necessary to reduce the loss of carbon reserves. According to the "14th Five-
466 Year Plan for National Economic and Social Development of Yunnan Province and the Outline
467 of the Visionary Goals for the Year 2035", Yunnan Province focused on "making new progress
468 in the building of eco-civilization by 2025, and building the vanguard of China's ecological
469 civilization by 2035". Responding climate change and achieving carbon peak and carbon
470 neutrality are also necessary for future development. Kunming needs to incorporate the dual-
471 carbon goal into the overall future development and foster comprehensive greener shift in
472 environmental development.

473 Based on the distribution of carbon sink in Kunming from 2000 to 2030 (Fig. 5), Luquan
474 County, Xundian County, and Dongchuan District in the north and Yiliang County and Shilin

475 County in the southeast were found to be the essential sources of carbon storage in Kunming.
476 The Luquan mountain area takes up 98.4% of the whole area of the county, and the forest
477 coverage rate is around 55.4%. Based on these advantages, forestry development and ecological
478 green development can be organically combined. Focusing on the positioning of the ecological
479 containment function area of Kunming, Luquan County, Xundian County, and Dongchuan
480 District need to strengthen ecological conservation construction and develop the Jiaozi Snow
481 Mountain Nature Reserve as an important water source conservation area and ecological
482 protection guard not only in Kunming but also the middle and upper reaches of the Yangtze
483 River. These areas should build a strong ecological security defense line in the north of
484 Kunming. As an 'ecological civilization county of Yunnan Province', Shilin County should lead
485 the construction of the national ecological civilization and help Yunnan in achieving its target of
486 'double carbon'. Considering that the tourism industry is important in Shilin County, eco-tourism
487 should be promoted to construct an ecological civilization. Yiliang County has an abundance of
488 forest resources and species diversity. The forest coverage rate of the county is 46.2%. Yiliang
489 County can utilize its resource advantages, strengthen the protection of forest resources based on
490 the current condition of forestry resources, simultaneously develop an ecological civilization and
491 forestry economy, and build an ecological security barrier with Shilin County in the southeast of
492 Kunming. Period 2000 to 2030, the carbon storage in the main urban area of Kunming City,
493 especially in the Dianchi Lake Basin, was found to decrease every year. Promoting the
494 ecological management of the Dianchi Lake Basin is imperative for the development of
495 Kunming City. The main urban area of Kunming City is located in the red line of water
496 conservation and eco-protection of plateau lakes and the upper reaches of the Niulan River.
497 Thus, its resource advantages need to be fully utilized to drive holistic and sustainable
498 development of the plateau lake basin. It is also necessary to improve the 'three lines and three
499 zones' delineation standards, strictly control the wetland parks and basic farmlands delineated in
500 the Dianchi Lake Basin, rationally conduct land and space planning, and enhance the efficiency
501 of land resources utilization. The ways to satisfy the requirements of urban expansion during
502 accelerated evolution and perform ecological protection need to be determined urgently for
503 developing Kunming City. Solving this problem is also the key to achieve the dual carbon goals
504 and the establishment of eco-civilization in Yunnan Province.

505 **Research prospect**

506 With the PLUS and InVEST models, the space-time changes in carbon storage in Kunming City
507 were predicted and evaluated, and the influence of land utilization conversion on carbon stock
508 was analyzed. The correlation between impervious surface coverage and vegetation index and
509 regional ecosystem carbon storage was analyzed. The findings provided new ideas for
510 sustainable development in the future. However, this study had some limitations. First, the
511 carbon storage calculation module of the InVEST model had certain shortcomings. Carbon stock
512 in the ecosystem is affected by many factors. The InVEST model considered land use change as
513 the only factor affecting carbon storage and ignored the effect of climate, topography, hydrology,
514 and other conditions. Additionally, the model also ignored the impact of interannual changes in

515 carbon density. Second, only 11 driving factors were considered when using the PLUS model for
516 future land cover; however, the actual land utilization evolution is affected by a large number of
517 physical and human factors. In future studies, the measured data might be used to determine the
518 dynamic carbon density. Besides land use, other influencing factors might be considered to
519 comprehensively evaluate the regional ecosystem carbon storage. While performing land-use
520 simulations, we should select as many driving factors as possible to predict future requirement of
521 land utilization and improve the prediction accuracy of future land utilization patterns.

522 **Conclusions**

523 Based on the data on land use and driving factors from 2000 to 2020, the PLUS and InVEST
524 models were used to monitor and study the time-space dynamics of land and ecosystem carbon
525 storage in Kunming from 2000 to 2030. The findings illustrated the following: (1) From 2000 to
526 2020, the land-use types in Kunming were mainly forest land. The total area of forest land,
527 grassland, and cultivated land decreased, and construction land increased. In the S1, the
528 construction land was predicted to expand greatly in 2030. In the S2, the forest land area was
529 predicted to increase greatly. In the S3, the cultivated land area was predicted to increase, the
530 construction land was predicted to increase moderately, and the forest land and grassland were
531 predicted to decrease slightly. (2) The carbon storage in Kunming showed a distribution pattern
532 of 'high in the north and low in the south'. The carbon storage of the ecosystem in 2000, 2010,
533 and 2020 was found to be 1.146×10^8 t, 1.139×10^8 t, and 1.120×10^8 t, respectively,
534 suggesting a continuous decrease. The carbon storage in 2030 was predicted to be 1.102×10^8 t
535 in S1, 1.136×10^8 t in S2, and 1.105×10^8 t in S3. (3) A significant spatial autocorrelation of
536 carbon storage was found in Kunming City. In the local space, the ecosystem carbon storage in
537 Kunming City from 2000 to 2020 was mainly characterized by the expansion of the coldspot
538 area. In 2030, the coldspot area was predicted to increase in the S1 scenario, slightly decrease in
539 the S2 scenario, and be similar to 2020 in the S3 scenario. (4) A global and local negative
540 correlation was found between impervious surface coverage and ecosystem carbon storage, and a
541 global and local positive correlation was found between NDVI and ecosystem carbon storage.

542 **Acknowledgements**

543 The authors gratefully acknowledge the support of their families and teachers to conduct this
544 comprehensive study.

545 **References**

- 546 Cai, W., & Peng, W. (2021). Exploring Spatiotemporal Variation of Carbon Storage Driven by
547 Land Use Policy in the Yangtze River Delta Region. *Land*, 10(11).
- 548 Cao, X. (2019). Geogovernance of national land use based on coupled human and natural
549 systems. *Journal of Natural Resources*, 34(10), 2051–2059.
- 550 Chen, B., Chen, F., Philippe, C., Zhang, H., Lv, H., Wang, T., Frédéric C., Liu Z., Yuan W. P.,
551 Wouter P. 2022. 'Challenges to China 's carbon neutrality in 2060: current status and
552 prospects', *Science Bulletin*, 67(20):2030–2035.

- 553 Chen, M., Wang, Q., Bai, Z., & Shi, Z. (2021). Transition of "Production-Living-Ecological"
554 Space and Its Carbon Storage Effect Under the Vision of Carbon Neutralization: A Case
555 Study of Guizhou Province. *China Land Science*, 35(11), 101–111.
- 556 Chen, Y., Yao, X., Ou, C., Zhang, Q., Yao, X. 2022. 'Response relationship between urban
557 spatial pattern and thermal environment : a case study of Hefei', *Environmental Science:*
558 1–15.
- 559 Cui, W., Cai, L., Xi, H., Yang, F., & Chen, M. (2022). Ecological security assessment and multi-
560 scenario simulation analysis of Zhejiang Greater Bay Area based on LUCC. *Acta*
561 *Ecologica Sinica*, 42(6), 2136–2148.
- 562 Ding, Q., Chen, Y., Bu, L., & Ye, Y. (2021). Multi-Scenario Analysis of Habitat Quality in the
563 Yellow River Delta by Coupling FLUS with InVEST Model. *International Journal of*
564 *Environmental Research and Public Health*, 18(5).
- 565 Ding, Y., Wang, L., Gui, F., Zhao, S., Zhu, W.. 2022. ' Ecosystem carbon storage around
566 Hangzhou Bay based on InVEST model and PLUS model', *Environmental Science:* 1–12.
- 567 Dorendorf, J., Eschenbach, A., Schmidt, K., & Jensen, K. (2015). Both tree and soil carbon need
568 to be quantified for carbon assessments of cities. *Urban Forestry & Urban Greening*,
569 14(3), 447–455.
- 570 Duan, P., Zhang, F., Liu, C. 2022. 'Impervious surface extraction and spatial difference analysis
571 of typical cities in Xinjiang based on Sentinel-2A/B', *Journal of Remote Sensing*,
572 26(07):1469–1482.
- 573 Fang, Y., Zu, J., Ai, D., Chen, J., & Liang, Q. (2021). Research on evaluation of the importance
574 of ecological protection in Kunming city oriented to spatial planning. *Journal of China*
575 *Agricultural University*, 26(3), 152–163.
- 576 Gao, J., Liu, L., Guo, L., Sun, D., Liu, W., Hou, W., Wu, S. 2022. 'Synergistic effects of climate
577 change and phenological changes on agricultural production and future food production
578 risks in the black soil region of Northeast China', *Geography*, 77(07):1681–1700.
- 579 Gao, L., Tao, F., Liu, R., Wang, Z., Leng, H., & Zhou, T. (2022). Multi-scenario simulation and
580 ecological risk analysis of land use based on the PLUS model: A case study of Nanjing.
581 *Sustainable Cities and Society*, 85.

- 582 Gogoi, A., Ahirwal, J., & Sahoo, U. K. (2022). Evaluation of ecosystem carbon storage in major
583 forest types of Eastern Himalaya: Implications for carbon sink management. *Journal of*
584 *Environmental Management*, 302.
- 585 Gong, W., Duan, X., Mao, M., Hu, J., Sun, Y., Wu, G., . . . Liu, T. (2022). Assessing the impact
586 of land use and changes in land cover related to carbon storage by linking trajectory
587 analysis and InVEST models in the Nandu River Basin on Hainan Island in China.
588 *Frontiers in Environmental Science*, 10.
- 589 Hanqiu, X. U. (2008). Comment on the Enhanced Water Index (EWI) : A Discussion on the
590 Creation of a Water Index. *Geo-information Science*, 10(6), 776–780.
- 591 Han-Qiu, X. U. (2009). Quantitative analysis on the relationship of urban impervious surface
592 with other components of the urban ecosystem. *Acta Ecologica Sinica*, 29(5), 2456–2462.
- 593 Ke, X., & Tang, L. (2019). Impact of cascading processes of urban expansion and cropland
594 reclamation on the ecosystem of a carbon storage service in Hubei Province, China. *Acta*
595 *Ecologica Sinica*, 39(2), 672–683.
- 596 Kong, J., Yang, R., Su, Y., & Fu, Z. (2018). Effect of land use and cover change on carbon stock
597 dynamics in a typical desert oasis. *Acta Ecologica Sinica*, 38(21), 7801–7812.
- 598 La, L., Gou, M., Li, L., Wang, N., Hu, J., Liu, C., & Xiao, W. (2021). Spatiotemporal Dynamics
599 and Scenarios Analysis on Trade-offs between Ecosystem Service in Three Gorges
600 Reservoir Area: A Case Study of Zigui County. *Journal of Ecology and Rural*
601 *Environment*, 37(11), 1368–1377.
- 602 Li, J., Xia, S., Yu, X., Li, S., Xu, C., Zhao, N., & Wang, S. (2020). Evaluation of Carbon Storage
603 on Terrestrial Ecosystem in Hebei Province Based on InVEST Model. *Journal of Ecology*
604 *and Rural Environment*, 36(7), 854–861.
- 605 Li, L., Song, Y., Wei, X., & Dong, J. (2020). Exploring the impacts of urban growth on carbon
606 storage under integrated spatial regulation: A case study of Wuhan, China. *Ecological*
607 *Indicators*, 111.
- 608 Li, R. W., Ye C. C., Wang Y., Han G. D., Sun J. 2021. 'Carbon storage estimation and driving
609 force analysis of the Tibetan Plateau based on InVEST model', *Grassland Journal*,
610 29(S1):43–51.

- 611 Li, W., Jia, S., He, W., Raza, S., Zamanian, K., & Zhao, X. (2022). Analysis of the consequences
612 of land-use changes and soil types on organic carbon storage in the Tarim River Basin
613 from 2000 to 2020. *Agriculture Ecosystems & Environment*, 327.
- 614 Li, X., Huang, C., Jin, H., Han, Y., Kang, S., Liu, J., . . . Sun, L. (2022). Spatio-Temporal
615 Patterns of Carbon Storage Derived Using the InVEST Model in Heilongjiang Province,
616 Northeast China. *Frontiers in Earth Science*, 10.
- 617 Liang, X., Guan, Q., Clarke, K. C., Liu, S., Wang, B., & Yao, Y. (2021). Understanding the
618 drivers of sustainable land expansion using a patch-generating land use simulation
619 (PLUS) model: A case study in Wuhan, China. *Computers Environment and Urban
620 Systems*, 85.
- 621 Lin, T., Yang, M., Wu, D., Liu, F., Yang, J., Wang, Y. 2022. 'Spatial Correlation and Prediction
622 of Carbon Storage in Guangdong Province Based on InVEST-PLUS Model',
623 *Environmental Sciences in China*: 1–17.
- 624 Luo, F., Ai, T., & Jia, X. (2022). Consistency Evaluation of Land Use Distribution Pattern
625 Supported by Spatial Autocorrelation. *Geomatics and Information Science of Wuhan
626 University*, 47(7), 1017–1024.
- 627 Rukeya, R., Alimujiang, K., Hirinayi, D., Wei, B., Zhang, X., Liang, H. 2022. 'Spatio-temporal
628 variation and prediction of carbon storage in urban agglomeration on the northern slope
629 of Tianshan Mountains', *Environmental Science of China*: 1–19.
- 630 Sarkodie, S. A., Owusu, P. A., & Leirvik, T. (2020). Global effect of urban sprawl,
631 industrialization, trade and economic development on carbon dioxide emissions.
632 *Environmental Research Letters*, 15(3).
- 633 Shao, Z., Chen R., Zhao, J., Xia C. Y., He, Y., Tang, F. 2022. 'Spatiotemporal evolution and
634 prediction of ecosystem carbon storage in Beijing based on FLUS and InVEST models',
635 *Ecology*, (23):1–14.
- 636 Song, Q., Feng, C., Ma, Z., Wang, N., Ji, W., & Peng, J. (2022). Simulation of land use change
637 in oasis of arid areas based on Landsat images from 1990 to 2019. *Remote Sensing for
638 Natural Resources*, 34(1), 198–209.
- 639 Sun, D., Liang, Y., 2021. Multi-scenario Simulation of Land Use Dynamic in the Loess Plateau
640 using an Improved Markov-CA Model. *J. Geo-Inform. Sci.* 23 (5), 825-836.

- 641 Tang, H., Xu, Y., Ai, J.. 2019. 'Carbon Storage and Carbon Density of Forest Vegetation and
642 Their Spatial Distribution Pattern in Yunnan Province', *Forestry Resource Management*,
643 (05): 37–43.
- 644 Tong, X., Zhang-Guo, Q., & Wei, Y. (2016). Remote Sensing Estimation of the Carbon Balance
645 Ability Based on the Object-Oriented Method for Guangxi Youjiang District. *Journal of*
646 *Geo-Information Science*, 18(12), 1675–1683.
- 647 Wang, J., & Zhang, Z. (2022). Land Use Change and Simulation Analysis in the Northern
648 Margin of the Qaidam Basin Based on Markov-PLUS Model. *Journal of Northwest*
649 *Forestry University*, 37(3), 139–148,179.
- 650 Wang, T., Gong, Z., & Deng, Y. (2022). Identification of priority areas for improving quality and
651 efficiency of vegetation carbon sinks in Shaanxi province based on land use change.
652 *Journal of Natural Resources*, 37(5), 1214–1232.
- 653 Xie, L., Xu, J., Zang, J., & Huang, T. (2022). Simulation and Prediction of Land Use Change in
654 Guangxi Based on Markov-FLUS Model. *Research of Soil and Water Conservation*,
655 29(2), 249–254,264.
- 656 Xiong, Y., Xu, W., Lu, N., Huang, S., Wu, C., Wang, L., . . . Kou, W. (2021). Assessment of
657 spatial?temporal changes of ecological environment quality based on RSEI and GEE: A
658 case study in Erhai Lake Basin, Yunnan province, China. *Ecological Indicators*, 125.
- 659 Xu, H., Wang, M., Shi, T., Guan, H., Fang, C., & Lin, Z. (2018). Prediction of ecological effects
660 of potential population and impervious surface increases using a remote sensing based
661 ecological index (RSEI). *Ecological Indicators*, 93, 730–740.
- 662 Yan, T., Peng, Y., Wang, X., Gong, H.. 2015. 'Estimation of Vegetation Carbon Storage and
663 Carbon Density of Forest Ecosystem in Yunnan Province', *Western Forestry Science*,
664 44(05): 62–67.
- 665 Yang, J. X., Liu M. M., Bi J. 2022. 'Climate Change Systemic Risk Perception and
666 Management', *Frontiers in Engineering Management Science*, 41(01):42–47.
- 667 Yang, L., Zhao, J., Zhu, J., Liu, L., Zhang, P. 2022. 'Spatiotemporal variation and prediction of
668 ecosystem carbon storage in Xi 'an based on PLUS and InVEST models', *Remote sensing*
669 *of natural resources*: 1–8.

- 670 Yang, S., Su, H., Zhao, G. 2022. 'Multi-scenario simulation of urban ecosystem service value
671 based on PLUS model-Taking Hanzhong City as an example', *Resources and*
672 *environment in arid areas*, 36(10): 86–95.
- 673 Yang, Y., Shi, Y., Sun, W., Chang, J., Zhu, J., Chen, L., . . . Fang, J. (2022). Terrestrial carbon
674 sinks in China and around the world and their contribution to carbon neutrality. *Science*
675 *China-Life Sciences*, 65(5), 861–895.
- 676 Zhang, H., Deng, W., Zhang, S., Peng, L., & Liu, Y. (2022). Impacts of urbanization on
677 ecosystem services in the Chengdu-Chongqing Urban Agglomeration: Changes and
678 trade-offs. *Ecological Indicators*, 139.
- 679 Zhang, L., Yue, X., Zhou, D., Fan, J., Li, Y. 2022. 'Effects of Climate Change and Human
680 Activities on Vegetation Restoration in Typical Steppe Region of China', *Environmental*
681 *Science*, 1–13.
- 682 Zhang, P., Geng, W., Yang, D., Li, Y., Zhang, Y., & Qin, M. (2020). Spatial-temporal evolution
683 of land use and ecosystem service value in the Lower Reaches of the Yellow River
684 Region. *Transactions of the Chinese Society of Agricultural Engineering*, 36(11), 277–
685 288.
- 686 Zhang, P., Li, Y., Yin, H., Chen, Q., Dong, Q., & Zhu, L. (2022). Spatio-temporal variation and
687 dynamic simulation of ecosystem carbon storage in the north-south transitional zone of
688 China. *Journal of Natural Resources*, 37(5), 1183–1197.
- 689 Zhang, T., Chang, J., Ma, Y., Sun, Y., Liu, C. 2022. 'Study on the evolution characteristics of
690 Bohai coastal wetland in Shandong and its correlation with human activities', *World*
691 *Geography Research*, 31(02): 329–337.
- 692 Zhang, X., & Gu, R. (2022). Spatio-temporal pattern and multi-scenario simulation of land use
693 conflict: A case study of the Yangtze River Delta urban agglomeration. *Geographical*
694 *Research*, 41(5), 1311–1326.
- 695 Zhang, X., Li, A., Nan, X., Lei, G., & Wang, C. (2020). Multi-scenario Simulation of Land Use
696 Change Along China-Pakistan Economic Corridor through Coupling FLUS Model with
697 SD Model. *Journal of Geo-Information Science*, 22(12), 2393–2409.
- 698 Zhao, Y., Qin, M., Pang, Y., Wang, Z., & Shi, Q. (2022). Evolution Simulation and Driving
699 Factors of Eco-spatial Carbon Sinks in Beibu Gulf Urban Agglomeration Based on
700 FLUS-InVEST Model. *Bulletin of Soil and Water Conservation*, 42(3), 345–355.

Table 1 (on next page)

Carbon density database of land use types in Kunming.

1 Table 1**2** Carbon density database of land use types in Kunming.

Land use	Aboveground carbon density	Underground carbon density	Soil carbon density	Carbon density of dead organic matter
Cultivated land	1.31	0.73	11.65	0
Forest land	40.41	10.45	42.75	2.62
Grassland	2.55	8.31	15.1	0.85
Water area	0	0	0	0
Construction land	0	0	0	0
Unused land	0	0	4.2	0

3

Table 2 (on next page)

Driving factors and data sources.

1 **Table 2**

2 Driving factors and data sources.

Data Type	Data Name	Resolution/m	Data Source
	GDP	1000	
	Population density	1000	Resource and Environment Science and Data Center, Chinese Academy of Sciences (https://www.resdc.cn/)
Social factors	Distance to government office	30	
	Distance to main road	30	Openstreetmap (https://www.openstreetmap.org/)
	Distance to highway	30	
	Elevation	30	Geospatial Data Cloud Official Website (https://www.gscloud.cn/)
	Slope	30	
Physical factors	Distance to water system	30	
	mean annual temperature	1000	Resource and Environment Science and Data Center, Chinese Academy of Sciences (https://www.resdc.cn/)
	mean annual rainfall	1000	
	Soil type	1000	

3

Table 3 (on next page)

Neighborhood weights of simulation scenarios.

1 Table 3**2** Neighborhood weights of simulation scenarios.

Scenarios	Cultivated land	Forest	Grassland	Water body	Construction land	Unused land
Trend continuation	0.50	0.77	0.50	0.58	0.83	0.50
Ecological protection	0.50	0.82	0.75	0.58	0.70	0.60
Comprehensive development	0.50	0.77	0.75	0.58	0.77	0.60

3

Table 4 (on next page)

Land utilization transfer matrix of Kunming from 2000 to 2020.

1 **Table 4**

2 Land utilization transfer matrix of Kunming from 2000 to 2020.

2020		Cultivated land	Forest land	Grassland	Water area	Construction land	Unused land	Total
Land use								
	Cultivated land	3426.40	218.07	196.14	25.74	387.23	0.80	4254.38
	Forest land	230.43	8765.48	441.07	40.69	119.74	1.79	9599.20
	Grassland	268.31	456.62	5154.64	19.52	236.11	6.52	6141.72
2000	Water area	17.92	4.07	6.27	420.81	24.26	0.32	473.65
	Construction land	32.26	11.51	10.47	4.20	425.58	0.19	484.21
	Unused land	0.99	1.17	4.18	0.51	0.13	60.91	67.89
	Total	3976.31	9456.92	5812.77	511.47	1193.05	70.53	21021.05

3

Table 5 (on next page)

Pearson correlation coefficient between carbon storage and impact factors in Kunming.

1 Table 5**2** Pearson correlation coefficient between carbon storage and impact factors in Kunming.

Impact factors	Impervious surface percentage	GDP	Population density	Elevation	NDVI	Average annual rainfall
carbon storage	-0.530	-0.2	-0.215	0.339	0.689	0.225

3

Table 6 (on next page)

Contribution of driving factors of land use.

1 **Table 6**

2 Contribution of driving factors of land use.

Driving factors	Land use					
	Cultivated land	Forest land	Grassland	Water area	Construction land	Unutilized land
DEM	0.111	0.183	0.1	0.136	0.085	0.111
GDP	0.166	0.091	0.133	0.187	0.143	0.166
Distance to government	0.093	0.091	0.104	0.022	0.104	0.093
Distance to highway	0.091	0.075	0.092	0.028	0.089	0.091
Population density	0.104	0.125	0.117	0.168	0.154	0.104
Average annual rainfall	0.089	0.081	0.089	0.069	0.111	0.089
Distance to main road	0.089	0.063	0.08	0.017	0.063	0.089
Distance to water system	0.079	0.071	0.104	0.097	0.069	0.079
Slope	0.078	0.117	0.084	0.2	0.096	0.078
Soil type	0.022	0.018	0.015	0.046	0.023	0.022
mean annual temperature	0.079	0.084	0.083	0.031	0.122	0.079

3

Figure 1

Study area.

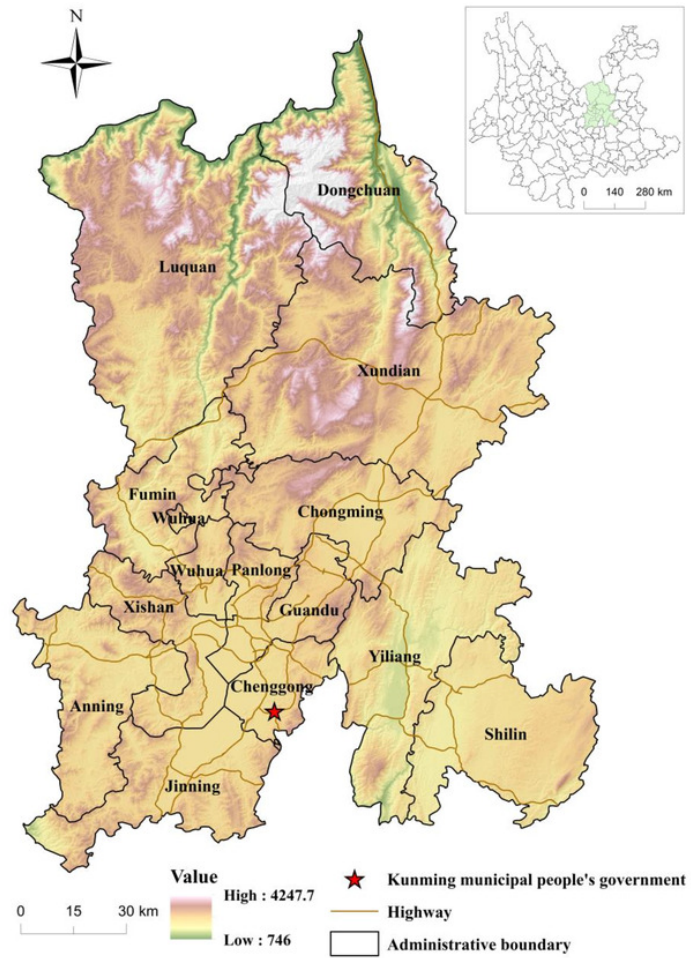


Fig.1. Study area.

Figure 2

Research framework.

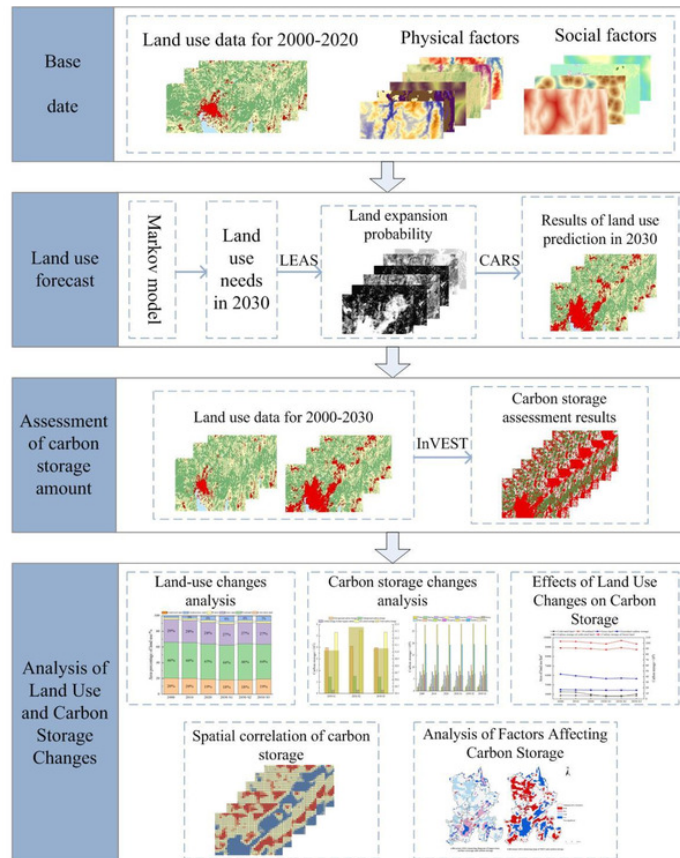


Fig.2. Research framework.

Figure 3

The overlay map of the area proportion of land utilization in Kunming from 2000 to 2030.

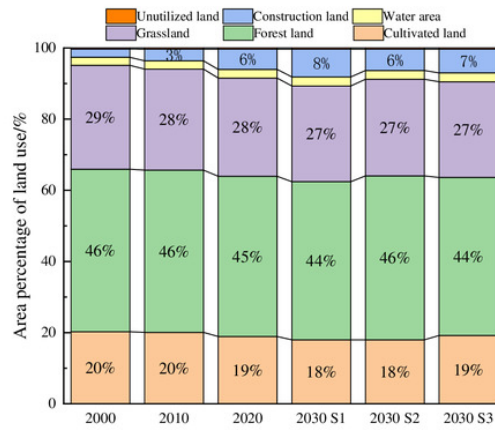


Fig.3. The overlay map of the area proportion of land utilization in Kunming from 2000 to 2030.

Figure 4

Land use changes in Kunming from 2000 to 2030.

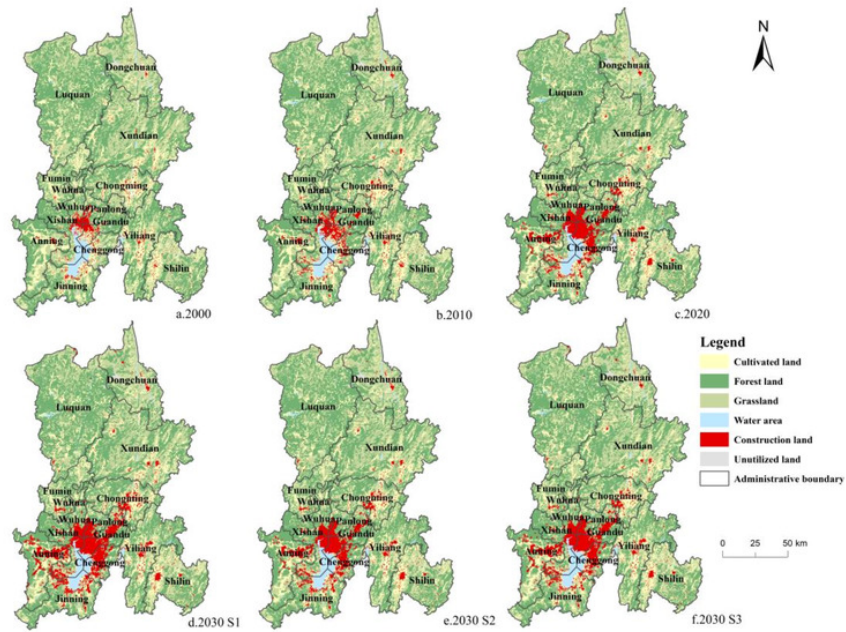


Fig.4. Land use changes in Kunming from 2000 to 2030.

Figure 5

Changes of carbon stock in Kunming under three development scenarios in 2030.

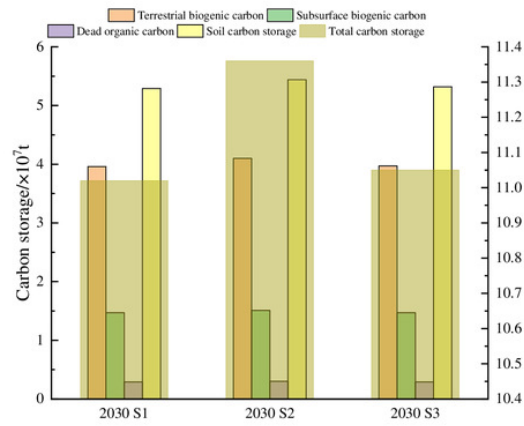


Fig.5. Changes of carbon stock in Kunming under three development scenarios in 2030.

Figure 6

Changes in carbon storage in Kunming from 2000 to 2030.

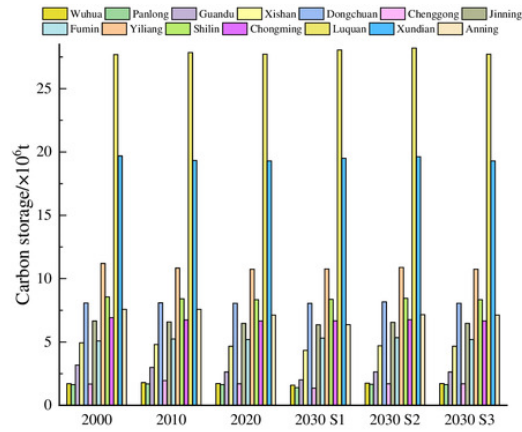


Fig.6. Changes in carbon storage in Kunming from 2000 to 2030.

Figure 7

Spatial distribution of carbon storage in Kunming from 2000 to 2030.

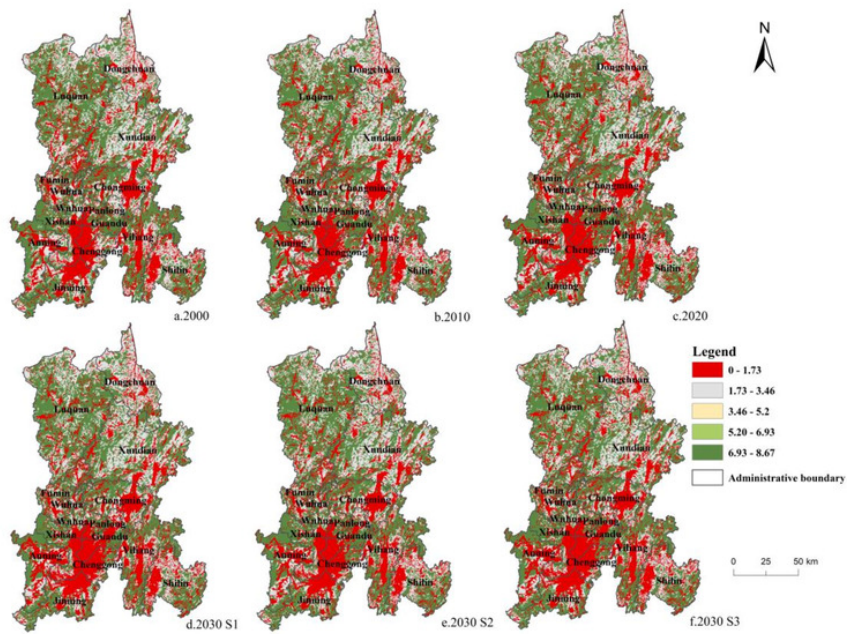


Fig.7. Spatial distribution of carbon storage in Kunming from 2000 to 2030.

Figure 8

Changes of main land types and carbon storage in Kunming from 2000 to 2030.

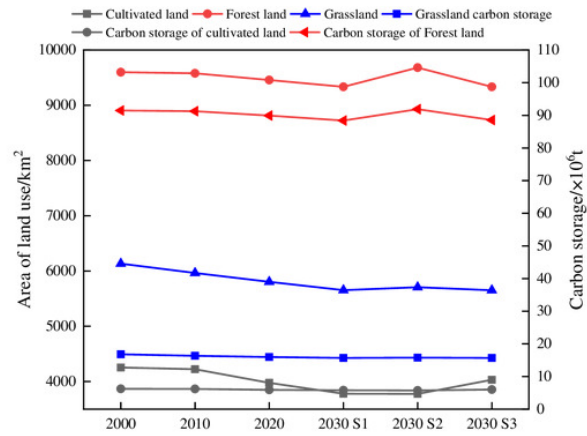


Fig.8. Changes of main land types and carbon storage in Kunming from 2000 to 2030.

Figure 9

Getis-Ord G_i^* analysis of carbon storage in Kunming from 2000 to 2030.

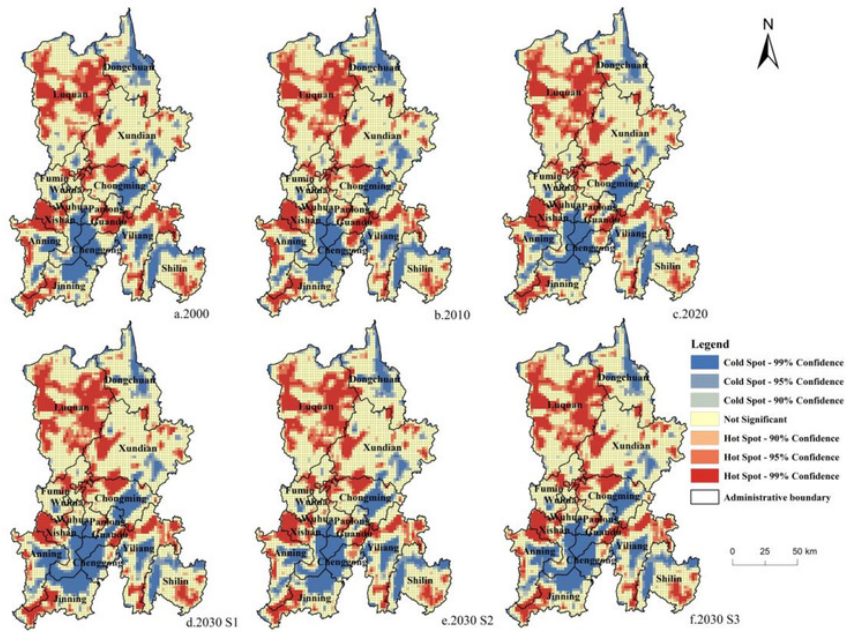


Fig.9. Getis-Ord G_i^* analysis of carbon storage in Kunming from 2000 to 2030.

Figure 10

Bivariate LISA cluster map of carbon storage and influencing factors in Kunming.

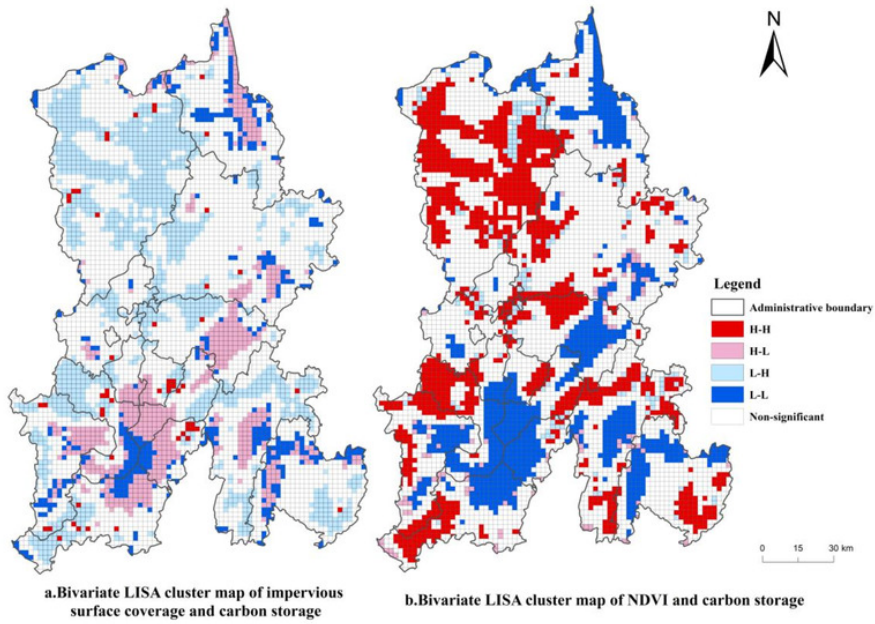


Fig.10. Bivariate LISA cluster map of carbon storage and influencing factors in Kunming.